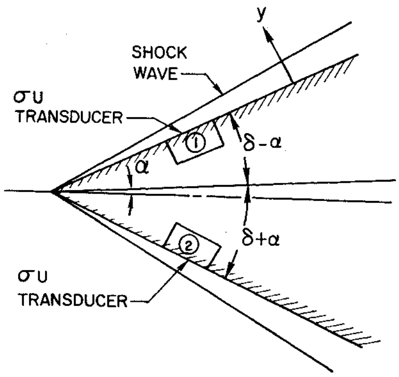

Fig. 1 The signal of transducer 2 is larger than that of transducer 1. The difference in signals can be used by the control system to properly activate the flaps or reaction jets.

Electrical conductivity σ was found from graphs appearing in the paper by Viegas and Peng.[4] The results are shown in Fig. 2 for five different altitudes. Each curve is shifted 2.5° to prevent overlapping the curves. On the windward side, increased deflection angle increases T and ρ, which, in turn, increase σ. However, the increased deflection angle decreases the flow velocity behind the shock wave. Increase in σ is relatively larger than the decrease in U, so that σU does increase as shown in Fig. 2.

Consider a wedge with half angle of 23.5° flying at zero angle of attack at 100,000 ft. The value of σU at the transducer is 3.6×10^3 mho/sec. Now assume an angle of attack of 1°. The transducer on the "windward" side (number 2 in Fig. 1) is exposed to a σU of 4.8×10^3, and the transducer on the "leeward" side sees σU of 2.3×10^3. The derivative of the fractional signal change is

$$\frac{\partial(\Delta e/e)}{\partial \alpha} = \frac{e_2 - e_1}{e\alpha} = \frac{4.8 - 2.3}{(3.6)(1°)} = \frac{0.69}{\text{deg}} \qquad (2)$$

There is a large change in signal for a change in angle of attack. Changes in signal level with changes in angle of attack have been observed in flight (see Fig. 10 of Ref. 2).

It is of interest to compare the fractional pressure change for the same conditions. For Newtonian flow, the pressure varies as the sine of the deflection angle squared. Hence, for the example,

$$\frac{\partial(\Delta p/p)}{\partial \alpha} = \frac{\sin^2 24.5° - \sin^2 22.5°}{\sin^2 23.5°} = \frac{0.16}{\text{deg}} \qquad (3)$$

For the example considered, the pair of σU transducers gives a larger fractional signal change than a pair of static pressure taps.

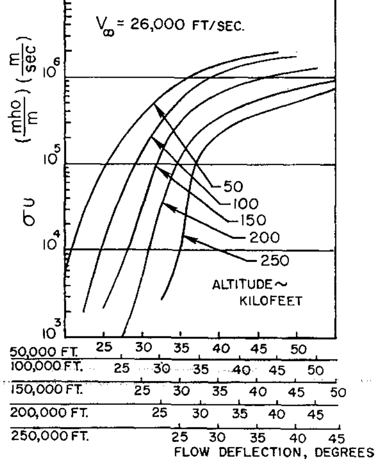

Fig. 2 Electrical conductivity/velocity for flow over a wedge as a function of deflection angle.

References

[1] Fuhs, A. E., "Flight instrumentation for reentry plasma sheath," *AIAA Proceedings of Fifth Biennial Dynamics Symposium*, edited by A. B. Cambel and T. P. Anderson (Northwestern University Press, Evanston, Ill., 1964), Chap. 19.

[2] Betchov, R., Fuhs, A. E., Meyer, R. X., and Schaffer, A. B., "Measurement of electrical conductivity of ionized air during reentry," Aerospace Eng. **21**, 54, 55, 68–83 (November 1962).

[3] Feldman, S., "Hypersonic gas dynamic charts for equilibrium air," Avco Research Lab., Res. Rept. 40 (January, 1957).

[4] Viegas, J. R. and Peng, T. C., "Electrical conductivity of ionized air in thermodynamic equilibrium," ARS J. **31**, 654–657 (1961).

A Family of Similar Solutions for Axisymmetric Incompressible Wakes

Toshi Kubota* and Barry L. Reeves†
California Institute of Technology, Pasadena, Calif.

AND

Harvey Buss‡
National Engineering and Science Company, Pasadena, Calif.

Introduction

In Ref. 1, Stewartson found a family of solutions of the Falkner-Skan equation

$$f''' + ff'' + \beta(1 - f'^2) = 0$$

for "free streamline" flows, i.e., with boundary conditions

$$(0) = f''(0) = 0; \quad \lim_{\eta \to \infty} f'(\eta) = 1$$

He showed that for positive pressure gradients $(-\frac{1}{2} < \beta < 0)$ the solutions exhibit a wake-like character $(f'(0) < 1)$ and that for $-0.1988 < \beta < 0, f'(0) < 0$. Recently it has been recognized[2] that these solutions, or actually their compressible analogs,[3] possess several important features displayed by flows in the base flow region or near wake of high speed objects.

In the present note, a new family of similar solutions is derived for axisymmetric, incompressible wakes. It is shown that, just as in the case of the two-dimensional Stewartson family, these solutions contain the Chapman[4] constant pressure mixing solution and the solution for uniform flow in the axial component of velocity as limiting cases.

Equations and Boundary Conditions

The continuity and momentum equations for large Reynolds number, incompressible axisymmetric flow are the following[5]:

$$\frac{\partial u}{\partial x} + \frac{1}{r}\frac{\partial(vr)}{\partial r} = 0 \qquad (1)$$

$$u\frac{\partial u}{\partial x} + v\frac{\partial u}{\partial r} = u_e\frac{du_e}{dx} + \frac{\nu}{r}\frac{\partial}{\partial r}\left(r\frac{\partial u}{\partial r}\right) \qquad (2)$$

Let

$$\psi = c_1 r x^m f(\eta) \qquad \eta = c_2 r/x^n \qquad (3)$$

Received April 14, 1964.

* Associate Professor of Aeronautics. Member AIAA.

† Research Fellow, Department of Aeronautics; also Consultant, National Engineering and Science Company. Member AIAA.

‡ Member of Technical Staff.

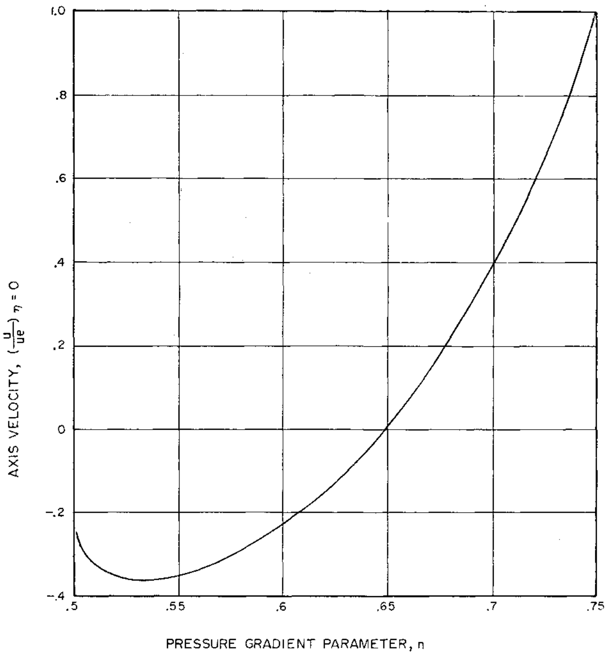

Fig. 1 Variation of velocity on wake axis with pressure gradient.

so that

$$u = \frac{1}{r}\frac{\partial\psi}{\partial r} = c_1c_2x^{m-n}\left[f' + \frac{f}{\eta}\right] \quad (4)$$

$$v = -\frac{1}{r}\frac{\partial\psi}{\partial x} = c_1x^{m-1}[n\eta f' - mf] \quad (5)$$

$$\frac{\partial u}{\partial r} = c_1c_2{}^2x^{m-2n}\left[f'' + \frac{1}{\eta}f' - \frac{1}{\eta^2}f\right] \quad (6)$$

By repeated differentiation of Eq. (4), the remaining terms of Eq. (2) can be found and substituted into the latter equation. For similarity, one then finds

$$m + n = 1$$

and if $c_1c_2 = u_0$, then

$$c_1 = (u_0\nu)^{1/2} \qquad c_2 = (u_0/\nu)^{1/2}$$

Equation (2) becomes

$$f''' + ff'' + (1 - 2n)(1 - f'^2) + \frac{2}{\eta}f'' - \frac{1}{\eta^2}f' + \frac{1}{\eta^3}f -$$

$$(1 - 4n)\frac{1}{\eta}ff' - 2(1 - n)\frac{1}{\eta^2}f^2 = 0 \quad (7)$$

The boundary conditions for wake flows are

$$y = 0{:}\ v = 0,\ \ \partial u/\partial r = 0;\ \ \lim_{y\to\infty} u = u_e$$

In terms of the nondimensional stream function, these boundary conditions can be written

$$\eta = 0{:}\ f(0) = f''(0) = 0$$
$$\lim_{\eta\to\infty}(f' + f/\eta) = 1 \qquad (\text{hence } u_e = u_0x^{m-n}) \quad (8)$$

Solutions

Solutions of Eq. (7) satisfying the boundary conditions (8) were obtained using a Runge-Kutta technique on an IBM 7090 computer. In order to start the solution for small $\eta(0 \leqslant \eta \leqslant 0.1)$ a power series of the form $f = \Sigma a_i\eta^i$ was assumed,

Table 1 Axisymmetric wake solutions

n	$(u/u_e)_{\eta=0}$	n	$(u/u_e)_{\eta=0}$
0.5025	−0.2525	0.68	0.2041
0.505	−0.2882	0.685	0.2443
0.5075	−0.3097	0.69	0.2865
0.51	−0.3245	0.695	0.3309
0.52	−0.3542	0.70	0.3774
0.53	−0.3621	0.705	0.4263
0.54	−0.3593	0.710	0.4776
0.55	−0.3493	0.713	0.5097
0.56	−0.3239	0.716	0.5429
0.57	−0.3139	0.720	0.5887
0.58	−0.2896	0.723	0.6242
0.59	−0.2612	0.726	0.6609
0.60	−0.2288	0.73	0.7117
0.61	−0.1932	0.733	0.7504
0.62	−0.1513	0.736	0.7912
0.63	−0.1058	0.74	0.8475
0.64	−0.0554	0.7425	0.8840
0.65	0.0002	0.745	0.9191
0.66	0.0617	0.7475	0.9576
0.67	0.1295	0.7488	0.9774
0.675	0.1659	0.7494	0.9876

and the a_i were determined from the boundary conditions and Eq. (7), i.e.,

$$a_k = 0 \qquad k \text{ even}$$
$$a_1 = f'(0)$$
$$a_3 = (1 - 2n)(4a_1{}^2 - 1)/16$$
$$a_5 = a_1a_3(1 - 4n)/12$$
$$a_7 = [a_3{}^2(1 - 4n) - 6a_1a_5]/36$$

With an assumed value of a_1, f and its derivatives were evaluated at $\eta = 0.1$, and the Runge-Kutta forward integration scheme was used to integrate Eq. (7) to some assigned value of η_∞. Then a_1 and η_∞ were modified until

$$(f' + f/\eta)_{\eta=\eta_\infty} = 1$$

$$\partial u/\partial r \sim (f'' + f'/\eta - f/\eta^2)_{\eta=\eta_\infty} < 10^{-4}$$

It is found that wake solutions $(u(0)/u_e \sim 2a_1 < 1)$ exist for $\frac{1}{2} < n < \frac{3}{4}$, where $n = \frac{1}{2}$ corresponds to Chapman's constant pressure mixing solution for flow over a step, and $n = \frac{3}{4}$ is the

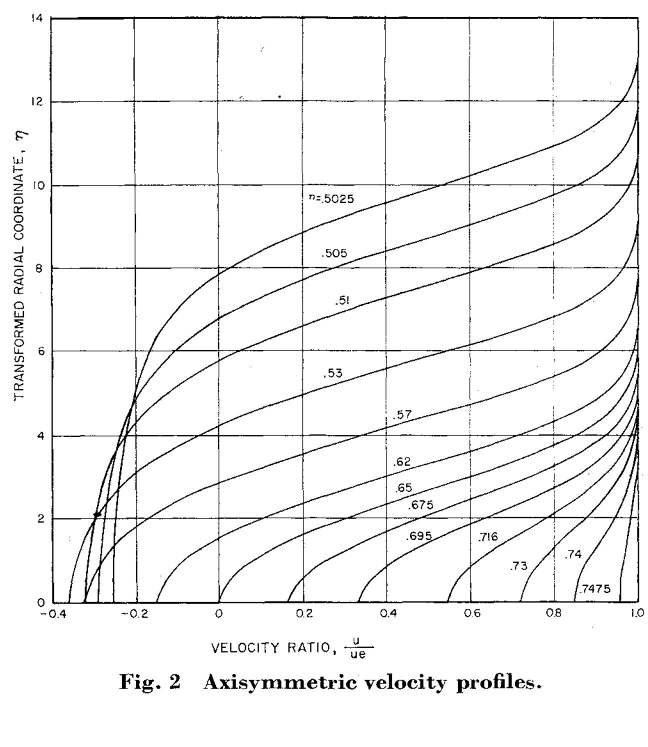

Fig. 2 Axisymmetric velocity profiles.

solution for uniform flow ($u/u_e = 1$), although in the latter case $v(y) \neq 0$ because of the positive pressure gradient. Figure 1 and Table 1 show the variation of the normalized velocity on the axis with the pressure gradient parameter n. The velocity on the axis vanishes for $n = 0.650$; hence this solution corresponds, at least conceptually, to the rear stagnation point found in steady wake flows.

The velocity profiles for various values of n are shown in Fig. 2. It is noteworthy that the present solutions for separated flow ($\frac{1}{2} < n < 0.648$) yield much larger back-flow velocities than do the two-dimensional solutions[3] and are apparently due to a "squeezing" effect that is a result of the axisymmetric geometry.

References

[1] Stewartson, K., "Further solutions of the Falkner-Skan equation," Proc. Cambridge Phil. Soc. **50**, 454–465 (1954).

[2] Lees, L. and Reeves, B. L., "Supersonic separated and reattaching laminar flows: I. General theory and application to adiabatic boundary layer-shock wave interactions," AIAA Preprint 64-4 (January 1964).

[3] Kennedy, E. D., "Wake-like solutions of the laminar boundary-layer equations," AIAA J. **2**, 225–231 (1964).

[4] Chapman, D. R., "Laminar mixing of a compressible fluid," NACA Rept. 958 (1950).

[5] Schlichting, H., *Boundary Layer Theory* (McGraw-Hill Book Co., Inc., New York, 1960), Chap. 10.

Analysis of MHD Channel Entrance Flows Using the Momentum Integral Method

W. Craig Moffatt*

Massachusetts Institute of Technology, Cambridge, Mass.

The use of integral methods for solution of the laminar boundary-layer equations is a widely accepted technique in ordinary hydrodynamics. In general, solutions are found by integrating the equations in two steps: first in the direction normal to the wall, using an assumed velocity distribution, and then in the flow direction, where a new dependent variable, the boundary-layer "thickness," arises as a result of the first integration. Such methods are of limited usefulness, since they give no indication of the detailed nature of the flow; however, they have proved to be of considerable value in assessing such effects as skin friction and heat transfer, the solutions for which prove to be relatively insensitive to the particular profiles assumed.

Several authors have attempted to apply integral methods to MHD flows, using simple parabolic[1, 2] or Karman-Pohlhausen[3] velocity distributions. Although these solutions show the correct qualitative behavior (eg., the asymptotic approach to a constant boundary-layer thickness when the magnetic field is applied normal to the surface and the flow), the quantitative results are suspect, primarily because of the assumed parabolic profile.

The success of such profiles in ordinary hydrodynamic entrance flows (e.g., Sparrow[4]) probably can be attributed to the fact that the asymptotic solution far from the channel entrance (plane Poiseuille flow) can be found exactly and yields a parabolic distribution. Correspondingly, it would be expected that the logical distribution to use for MHD entrance

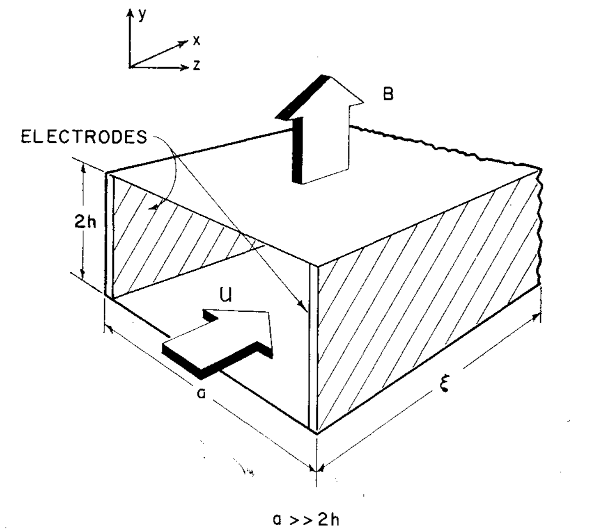

Fig. 1. Schematic diagram of entrace to MHD channel. The value of $K = E/UB$ is determined by the nature of the external electrical connection between the electrodes.

flows would be the asymptotic solution for the magnetic case, i.e., Hartmann flow.

Several authors have treated these flows using other techniques. For example, Roidt and Cess,[5] following a method developed by Schlichting for nonmagnetic flow, divided the entrance region into two sections, an upstream section where the solution was patterned after the Blasius series solution, and a downstream section where the velocity was expressed as the fully developed profile plus a deviation velocity. On the other hand, Shohet et al.[6] solved the entrance region problem numerically by writing the momentum and continuity equations in a stable finite difference form. The purpose of this note is to present the results of a solution based on the momentum integral method using an assumed Hartmann-like velocity distribution.

For fully developed, incompressible, steady flow of an electrically conducting fluid at low magnetic Reynolds number in the channel shown in Fig. 1, the x-momentum equation becomes

$$(dp/dx) + jB - \mu(d^2u/dy^2) = 0 \qquad (1)$$

where, in the absence of Hall effects,

$$j = \sigma(uB - E) \qquad (2)$$

In these equations, j is the current density, σ the electrical conductivity of the fluid, and B and E the imposed magnetic and electric field strengths, respectively. These equations can be readily solved (see, for example, Ref. 7) to yield

$$u = \left(\frac{E}{B} - \frac{dp/dx}{\sigma B^2}\right)\left[1 - \frac{\cosh\{M(1 - y/h)\}}{\cosh M}\right] \qquad (3)$$

where $M = Bh(\sigma/\mu)^{1/2}$ is the Hartmann number. Since the first bracketed term in Eq. (3) is constant for fully developed flow, a dimensionless velocity distribution

$$\frac{u}{u_c} = \frac{\cosh M - \cosh\{M(1 - y/h)\}}{\cosh M - 1} \qquad (4)$$

can be formed, where u_c is the velocity at the center of the channel.

The momentum and continuity equations for boundary layers on the nonconducting walls of the channel shown in Fig. 1 may be written as

$$u\frac{\partial u}{\partial x} + v\frac{\partial u}{\partial y} = -\frac{1}{\rho}\frac{\partial p}{\partial x} - \frac{jB}{\rho} + \frac{\mu}{\rho}\frac{\partial^2 u}{\partial y^2} \qquad (5)$$

$$(\partial u/\partial x) + (\partial v/\partial y) = 0 \qquad (6)$$

Received April 15, 1964. This work was performed under the auspices of Project SQUID, Nonr-3623(S-2). The facilities of the Massachusetts Institute of Technology Computation Center were used for the numerical calculations.

* Assistant Professor of Mechanical Engineering. Member AIAA.